ELSEVIER

Cardiovascular Research 69 (2006) 825 – 835

Cardiovascular Research

www.elsevier.com/locate/cardiores

Caveolae and sarcoplasmic reticular coupling in smooth muscle cells of pressurised arteries: The relevance for Ca^{2+} oscillations and tone

Linda Shaw [a], Michele A. Sweeney [b], Stephen C. O'Neill [a], Carolyn J.P. Jones [b], Clare Austin [a], Michael J. Taggart [a,b,*]

[a] *Division of Cardiovascular and Endocrine Sciences, University of Manchester, Great Britain, United Kingdom*
[b] *Division of Human Development, University of Manchester, Great Britain, United Kingdom*

Received 12 September 2005; received in revised form 1 December 2005; accepted 20 December 2005

Time for primary review 29 days

Abstract

Objective: A close association of caveolae and sarcoplasmic reticulum (SR) has been suggested to be important for contractile activation of smooth muscle. Here, we investigate the presence of such arrangements in pressurised resistance arteries and examine the influence of two agents purported to disrupt caveolae and/or SR conformations by different mechanisms of action.
Methods: Rat mesenteric small arteries (RMSA) were mounted on a pressure myograph and the functional (lumen diameter and Ca^{2+} oscillations) and ultrastructural effects of the phosphatase inhibitor calyculin-A (cal-A), or the cholesterol binding agent methyl-β-cyclodextrin (mβcd), examined by light and electron microscopy.
Results: Smooth muscle cells of RMSA exhibited a prominent peripheral SR that often encircled individual caveolae. The peripheral SR on occasion was observed to make contact with centrally located SR allowing for a structural association of caveoale–SR–myofilaments. Cal-A maximally constricted RMSA and disrupted the regular SR–caveolae appearance such that concentrated swirls of SR not enveloping caveolae were evident. Mβcd treatment, in contrast, inhibited agonist contractility and reduced the appearance of caveolae whilst peripheral SR apposition to the plasmalemma could still be observed. Treatment with either agent inhibited agonist-mediated smooth muscle Ca^{2+} oscillations.
Conclusion: We present data that supports a structural arrangement of caveolae and underlying peripheral SR in smooth muscle cells of pressurised resistance arteries that serves to regulate Ca^{2+} oscillations and contractile activation.

Keywords: Caveolae; Sarcoplasmic reticulum; Resistance arteries; Ca oscillations

1. Introduction

Considerable support has grown for a role of caveolae, Ω-shaped invaginations of the plasma membrane, in the regulation of smooth muscle contractile activation [1–3]. The distinct morphological appearance of caveolae arises from the interaction of caveolin proteins with cholesterol and sphingolipids. Caveolins may participate in the co-ordination of signal transduction pathways by their ability to bind to and/or alter the activation of a variety of intracellular signal transduction molecules [4]. The enrichment of particular receptors, channels and proteins in caveolae may facilitate the regulation of cellular excitability from within these microdomains [3–11]. This, and the positioning of caveolae in relation to other intracellular structures, may impart a direct role in the transmission of Ca^{2+} signals regulating force production. In this context, depletion of cholesterol from smooth muscle has been reported to alter the occurrence of Ca^{2+} sparks and store-operated Ca^{2+} entry [8,12].

* Corresponding author. Smooth Muscle Physiology Group, Division of Cardiac and Endocrine Sciences, Department of Medicine, University of Manchester, Manchester Royal Infirmary, Oxford Road, Manchester, M13 9WL, United Kingdom. Tel.: +44 161 276 5469; fax: +44 161 276 8433.
E-mail address: Michael.j.Taggart@manchester.ac.uk (M.J. Taggart).

0008-6363/$ - see front matter © 2006 European Society of Cardiology. Published by Elsevier B.V. All rights reserved.
doi:10.1016/j.cardiores.2005.12.016

In recent years, it has become evident that excitatory agonists that tonically constrict smooth muscle, do so by regulating the temporal and/or spatial characteristics of Ca^{2+} oscillations of individual cells [13–18]. Such oscillations commonly take the form of waves of Ca^{2+} originating in one point of the cell, propagating a distance of many tens of microns and lasting 2–6 s. These Ca^{2+} waves may be modulated by Ca^{2+} entry mechanisms and are stimulated in smooth muscle cells of many tissues by a variety of receptor-mediated agonists (for reviews see Refs. [19,20]). In freshly isolated single smooth muscle cells, the propagated Ca^{2+} waves have been suggested to involve IP_3-induced Ca^{2+} release from the sarcoplasmic reticulum (SR) either exclusively, or with the involvement of ryanodine-sensitive calcium-induced calcium release [21–23]. In resistance arteries the regulation of vessel diameter will be critically dependent upon this governance of Ca^{2+} dynamics in individual smooth muscle cells. The dose-dependent constriction of pressurised rat mesenteric arteries is associated with elevations in (i) the number of smooth muscle cells exhibiting Ca^{2+} oscillations; (ii) the frequency of oscillations per individual cell [18,24]. Here too, the SR appears critical as pharmacological modulators of SR Ca^{2+} homeostasis alter the dynamics of Ca^{2+} waves in intact isobaric arteries [25,26]. Therefore, an important determinant of the characteristics of Ca^{2+} oscillations, and whether they will be able to activate myofilament contraction in smooth muscle cells of resistance arteries, will be the spatial distribution of SR. In many smooth muscles, a close link between caveolae and SR at the cell periphery has been reported (Ref. [19] for review). In particular, a recent structural study of non-vascular bladder smooth muscle suggested that co-localisation of SR proteins and the L-type Ca^{2+} channel in caveolar domains may contribute to the organisation of functional Ca^{2+} release sites [3]. However, given this, it is surprising that

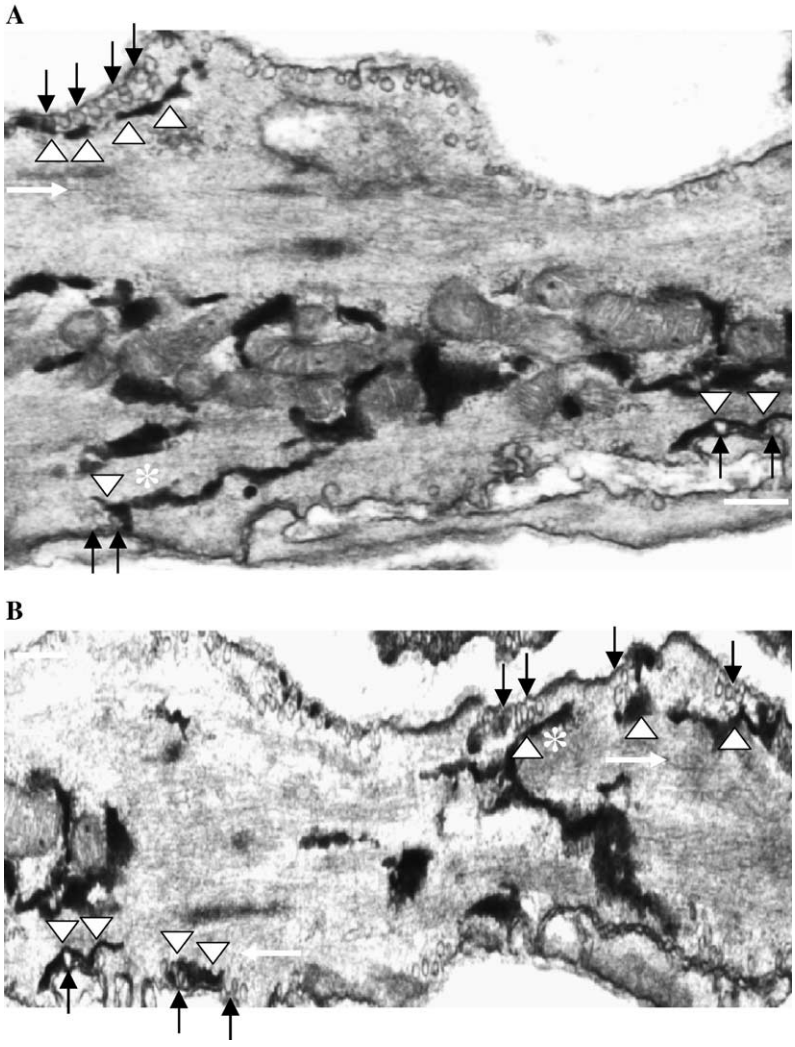

Fig. 1. Arrangement of caveolae and sarcoplasmic reticulum in smooth muscle cell of pressurised arteries. (A, B) EM examination (longitudinal sections) of smooth muscle cells of a pressurised artery fixed whilst contracted maximally to phenylephrine. Caveolae denoted by black arrows are in close apposition to peripheral black-stained SR marked by white arrowheads. In the positions marked by white asterisks, peripheral SR strands close to caveolae are seen to connect to centrally positioned SR. White arrows indicate myofilaments. The latter interweaves close to mitochondria. Scale bars = 200 nm.

detailed ultrastructural information on the intracellular distribution of the SR in relation to caveolae in resistance vessels is scant.

In this study, therefore, we use electron microscopy to report the spatial arrangement of caveolae and SR in smooth muscle cells of pressurised rat mesenteric small arteries. Furthermore, we make use of two agents that, by different mechanisms of action, are suggested to disrupt caveolae and/or peripheral SR arrangements: (i) The phosphatase inhibitor calyculin-A has recently been suggested to alter peripheral SR–plasmalemmal couplings in venous smooth muscle [27] and another serine/threonine phosphatase inhibitor results in caveolae internalisation in several cultured cells [28–30]. (ii) The cholesterol sequestering agent methyl-β-cyclodextrin (mβcd) has been reported to disrupt caveolae in many smooth muscle preparations [4,8,9]. Thus, both these agents, although acting by different cellular mechanisms, may alter the structural relationship between caveolae and SR (and myofilaments). We examine this in the present study and relate it to agonist-mediated changes in $[Ca^{2+}]_i$ oscillations and vessel diameter. Our data suggests that caveolae and peripheral SR in smooth muscle cells of pressurised resistance arteries are arranged in a manner that serves to facilitate the generation and propagation of Ca^{2+} waves and subsequent regulation of vasomotor tone.

2. Methods

2.1. Rat mesenteric resistance artery isolation and cannulation

The investigation conforms with the *Guide for the Care and Use of Laboratory Animals* published by the US National Institutes of Health (NIH Publication No. 85-23, revised 1996). Male Wistar rats (250–300 g) were killed by stunning followed by cervical dislocation. The mesentery was removed and placed in ice-cold physiological salt solution (PSS) of composition (in mmol/l): NaCl 119, KCl 4.7, $MgSO_4 \cdot 7H_20$ 1.2, $NaHCO_3$ 25, KH_2PO_4 1.17, K_2EDTA 0.03, glucose 5.5, $CaCl_2 \cdot 2H_20$ 1.6 at pH 7.4. A 3rd or 4th order mesenteric artery (2–3 mm in length) was dissected from each animal and placed in PSS within a bath chamber of a pressure myograph (model CH/1 or CH/1/QT, Living Systems Instrumentation, USA), cannulated onto two glass micropipettes (tip diameters 30–50 μm) as described

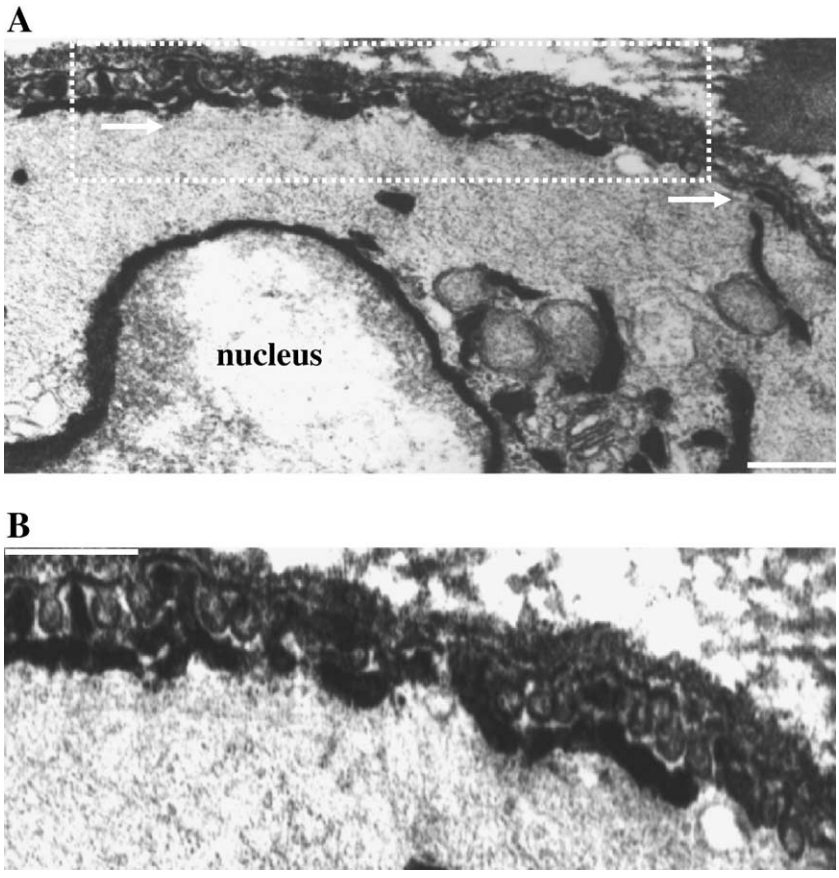

Fig. 2. Caveolae and peripheral SR distributions. (A) A transverse section of pressurised artery indicating prominent peripheral SR in close juxtaposition to caveolae of the plasma membrane as well as central SR close to mitochondria and the nucleus. Scale bar=200 nm. (B) Enlargement of the area denoted by the dotted box in panel A further indicates the close proximity of peripheral SR to caveolae; this peripheral SR is often observed enveloping the caveolae. White arrows indicate myofilaments. Scale bar=200 nm.

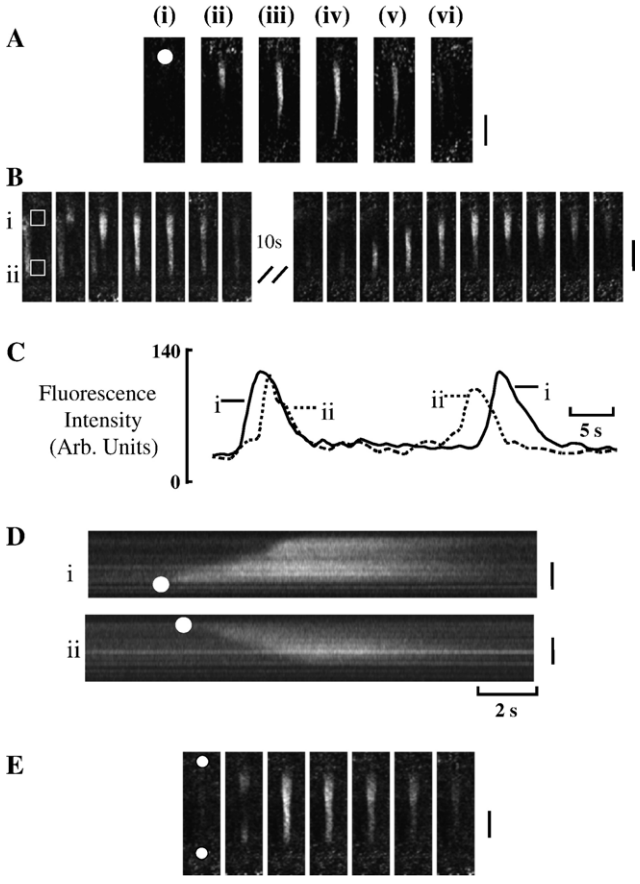

Fig. 3. Smooth muscle cellular $[Ca^{2+}]_i$, changes in response to different agonists. Laser scanning confocal microscopy of pressurised vessels revealed several patterns of $[Ca^{2+}]_i$ waves of individual smooth muscle cells to phenylephrine (10 μM). (A) Panels (i)–(vi) illustrate consecutive (1 s between images) changes in smooth muscle cell $[Ca^{2+}]_i$ in the form of a wave propagated from one end of the cell (indicated by white dot). (B) Separate $[Ca^{2+}]_i$ waves travelling in opposite directions in the same cell. The cell in question is indicated in the first frame by two white boxes marked i and ii. A $[Ca^{2+}]_i$ wave began in the top portion of the cell and, in consecutive frames (1 s), travelled progressively downwards to the bottom of the cell. In the same cell (dotted lines indicate a 10 s break in recording) in the continued presence of phenylephrine, a $[Ca^{2+}]_i$ wave originated in the bottom portion of the cell and progressed in consecutive frames towards the top of the cell. (C) Continuous line-plots of the $[Ca^{2+}]_i$ changes (including the 10 s break of panel A) recorded from the ROI marked by the white boxes in panels A. The solid trace refers to the time-course of the $[Ca^{2+}]_i$ wave in box (i) and the dotted line illustrates the time-course of the $[Ca^{2+}]_i$ wave in box (ii). The first $[Ca^{2+}]_i$ wave clearly passes box (i) before reaching box (ii). In contrast, the second wave of $[Ca^{2+}]_i$ passes box (ii) before reaching box (i). (D) Linescan confocal images of a separate smooth muscle cell of an artery also illustrating progression of separate $[Ca^{2+}]_i$ waves (initiated at points indicated by white spot) in opposite directions. (E) Illustration of a $[Ca^{2+}]_i$ wave originating in two distinct regions of the cell, as indicated by the two white circles at the top and bottom, and progressing towards each other. Panels A–B, D–E scale bars = 20 μm.

previously [18] and pressurised to 50 mm Hg using a pressure servo-control unit (Living Systems Instrumentation, USA). The arteriograph was placed on top of a Nikon Diaphot 200 microscope and viewed with a ×10 objective. Lumen diameters were measured using a video image analyser and contractile responses to the α-adrenoceptor agonist phenylephrine (10^{-9}–10^{-5} mol/l), the thromboxane mimetic U46619 (10^{-9}–10^{-6} mol/l) or high K^+ solution (isosomotically substituted for NaCl) assessed.

2.2. Arterial diameter measurements following treatment with calyculin-A or mβcd

Arteries were treated for 15 min with 2×10^{-6} mol/l of the phosphatase inhibitor calyculin-A, washed for 15 min and then stimulated with 10^{-5} mol/l phenylephrine or 10^{-6} mol/l U46619. In a separate set of experiments, arteries were treated with 10^{-2} mol/l mβcd for 1 h, the agent washed off and, 15 min later, the contractile response to a single dose of 10^{-5} mol/l phenylephrine assessed. Following washout, a concentration–response curve to phenylephrine (10^{-9}–10^{-5} mol/l) was performed. The contractile responses of other arteries similarly treated by mβcd to a single dose (10^{-6} mol/l) and cumulative doses of U46619 (10^{-9}–10^{-6} mol/l) were also assessed.

In a separate set of experiments, the influence on function and structure of mesenteric arteries of replenishing cholesterol to mβcd-treated tissues was established. Following mβcd treatment, arteries were exposed to a single dose of 10^{-5} mol/l phenylephrine; after 5 min, this was supplemented with 0.5 mM free cholesterol for 20 min and diameter changes compared to that observed to phenylephrine in the same vessels before mβcd exposure.

2.3. Electron microscopy of pressurised vessels

Vessels were mounted in arteriograph model CH/1/QT if to be prepared for electron microscopy by rapid rotation through 180° and immersion in fixative (~2 s, 2.5% gluteraldehyde in 0.1 M sodium cacodylate pH 7.3) whilst all the while remaining pressurised. Following 30 min equilibration, vessels were stimulated with phenylephrine (10^{-5} mol/l) to check for contractile viability and returned to PSS. Arteries were fixed following treatment and washout of calyculin-A or mβcd (as above) and compared to fixed arteries that had not been exposed to calyculin-A nor mβcd. The arteries were incubated in this fixative at room temperature for 3 h, washed several times in 10^{-1} mol/l sodium cacodylate buffer, to which 3×10^{-3} mol/l $CaCl_2$ had been added, and stored at 4 °C. Approximately 0.5 mm thick sections of vessel were post-fixed in the dark (2 h, room temperature) in 2% osmium tetroxide in 10^{-1} mol/l sodium cacodylate buffer to which was added 0.8% (w/v) potassium ferricyanide [31,32]. Tissues were block stained with 2% aqueous uranyl acetate (90 min), dehydrated in an ascending alcohol series, treated with propylene oxide and embedded in Taab epoxy resin in Beem capsules or rectangular moulds. Ultrathin sections of transverse or longitudinal orientation to the vessel lumen were cut with a diamond knife, mounted on copper grids and stained with lead citrate. Specimens were examined in a Philips EM 301 electron microscope at an accelerating voltage of 60 kV.

2.4. Measurement of arterial smooth muscle cell $[Ca^{2+}]_i$ signals

Measurements of global vessel wall $[Ca^{2+}]_i$ were performed as described previously in pressurised mesenteric arteries [18]. Arteries were loaded with 20 μM of the membrane-permeant acetoxymethylester form of the ratiometric calcium-sensitive dye Indo-1 for 3 h in Hepes-buffered salt solution (in mM: NaCl 154, KCl 5.4, $MgSO_4$ 1.2, glucose 10, $CaCl_2$ 10, Hepes 10, pH 7.4 with NaOH) at room temperature. Following washing with PSS, the vessels were mounted on a Nikon Diaphot 200 inverted microscope, viewed with a ×10 Fluor objective (via a 600 nm filter), excited at 340 nm and emissions at 400 and 500 nm recorded as an indicator of $[Ca^{2+}]_i$.

For experiments involving measurement of cellular $[Ca^{2+}]_i$ by laser scanning confocal microscopy the arteriograph chamber model CH/1 had cannulae between securable jaws at a slight angle (~10°) to allow positioning of the vessel wall close to the bottom of the microscope slide. Arteries were incubated with the membrane-permeant acetoxymethylester form of the calcium-sensitive dye Fluo-3 (15×10^{-6} mol/l, Molecular Probes) for 3 h in Hepes-buffered salt solution. The arteriograph was placed on a Nikon Diaphot 300 inverted microscope attached to a Bio-Rad MRC 1024 confocal laser scanning head and viewed with a ×60 Fluor water objective (N.A. 1.2). Tissues were constricted with 3×10^{-7}–10^{-5} mol/l phenylephrine or 10^{-6} mol/l U46619 and changes in individual cellular $[Ca^{2+}]_i$ measured as detailed in Ref. [18]. Fluo-3 fluorescence was excited at 488 nm with a Kr/Ar laser source (100 mW) and fluorescence >515 nm emitted in the confocal plane collected by a photomultiplier tube and digitally recorded with Bio-RAD Lasersharp software. Whole field optical scans in the same *z*-plane of focus were taken every 1 s. Off-line analysis of stored images was performed with *Image* J software (Version 1.27z). A region of interest (ROI) was described within individual cells in confocal images, positioned such that the ROI always remained within

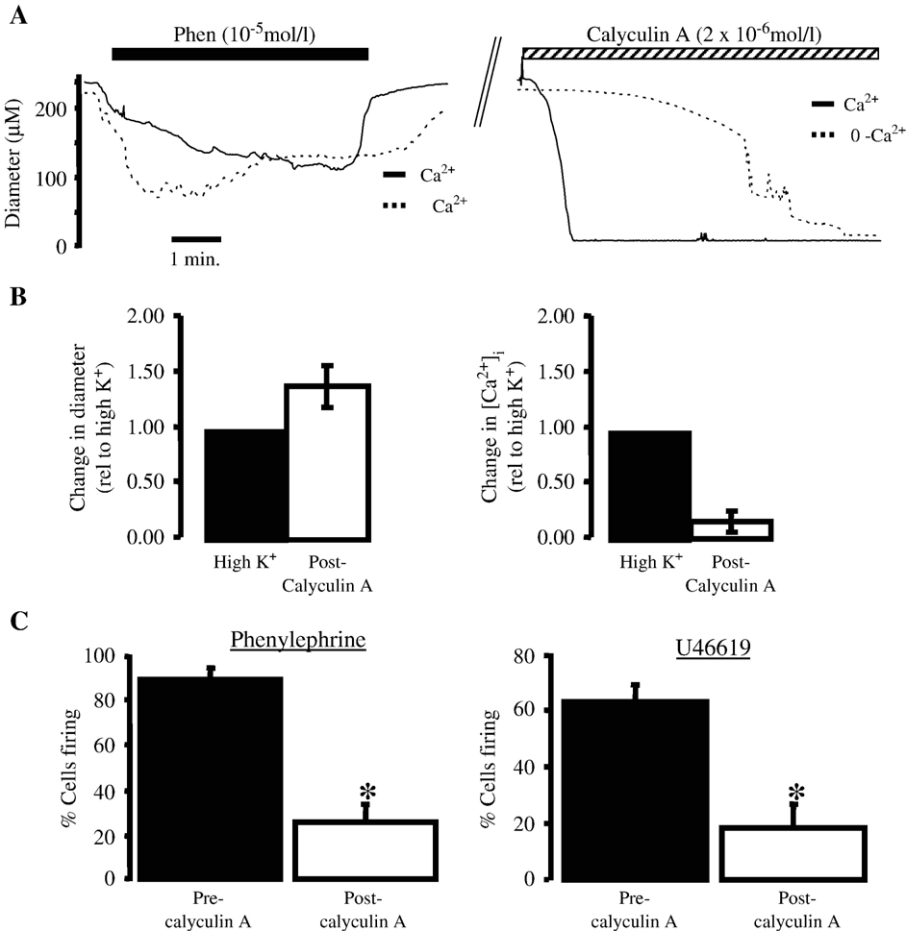

Fig. 4. Calyculin-A effects on pressurised artery diameter global $[Ca^{2+}]_i$ and $[Ca^{2+}]_i$ oscillations. (A) Calyculin-A (2×10^{-6} mol/l) resulted in constrictions, both in the presence and absence of Ca^{2+}, that were greater than those to 10^{-5} mol/l phenylephrine obtained in the same tissues in the presence of Ca^{2+}. (B) Although the mean change in diameter following calyculin-A application was greater than that due to addition of high K^+ solution, the change in global $[Ca^{2+}]_i$ was not elevated above basal. (C) Following calyculin-A treatment, the percentage of cells exhibiting Ca^{2+} oscillations in response to phenylephrine (25±8.0% of 83 cells from 6 vessels) or U46619 (63±5.8% of 172 cells from 11 vessels) was markedly reduced (open bars) compared to before treatment (black bars, 88±5.0% of 80 cells from 6 vessels for PE and 20±7.5% of 86 cells from 5 vessels for U46619). At rest, the number of cells exhibiting Ca^{2+} oscillations was also reduced from 19% to 3%.

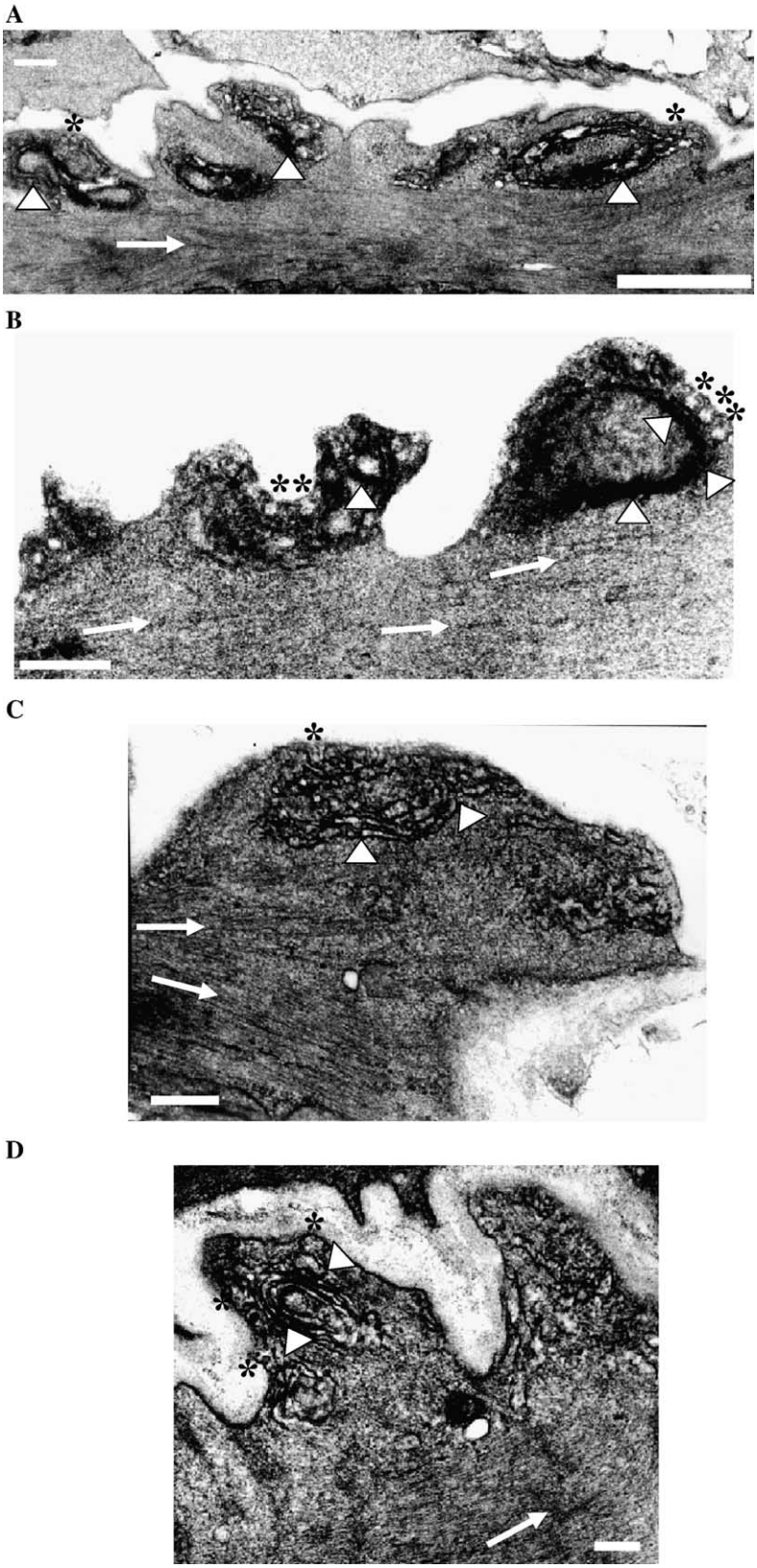

Fig. 5. Effects of calyculin-A on the ultrastructure of isolated pressurised arterial smooth muscle. A, B and C demonstrate that calyculin-A treatment resulted in the appearance of prominent membrane notches. These contained caveolae (asterisks) and swirls of SR (denoted by white triangles) that were no longer in close apposition to caveolae. Some indication of invagination of caveolae is evident. White arrows show the directions of the myofilaments. Tissues were treated with calyculin-A in the presence (A–C) or absence (D) of extracellular Ca^{2+}. White arrows indicate myofilaments. Scale bars = 800 nm (A) and 200 nm (B–D).

an identified cell. The software calculated the average ROI fluorescence value to follow Ca^{2+} alterions with time in individual cells. Similarly, in selected individual cells, the linescan mode of laser excitation allowed the time-course of Ca^{2+} oscillations to be monitored.

2.5. Drugs and chemicals

All drugs and chemicals, with the exception of indo-1(AM) and Fluo-3(AM) (Molecular Probes), gluteraldehyde and osmium tetroxide (Agar Scientific Ltd), potassium ferricyanide (BDH) and epoxy resin (Taab Laboratories Equipment, Aldermarston) were obtained from Sigma. Fluo 3(AM) and indo-1(AM) were dissolved in Pluronic F-127 20% solution in DMSO (obtained from Molecular Probes) to give 10^{-3} mol/l stock solutions. A 10^{-2} mol/l stock solution of U46619 was made by dissolving in a mixture of 100% ethanol and 1 mg kg^{-1} sodium carbonate (1:2). PE was dissolved in PSS. Cholesterol PEG 600 (Sigma UK catalogue number C1145) was a polyoxyethyl–cholesterol sebacate, a water soluble complex containing at least 20% cholesterol (batch-dependent). A stock solution of 60 mg/ml complex was dissolved in PSS and further diluted to a final bath concentration of 0.5 mM cholesterol.

3. Results

3.1. Electron microscopic examination of caveolae and SR in smooth muscle cells of pressurised arteries

The smooth muscle cells of pressurised arteries, 2–4 layers deep, were predominantly circular in orientation wrapping around the vessel wall. Ultrastructural examination of these smooth muscle cells revealed abundant plasmalemmal caveolae appearing singularly or in rows (Figs. 1 and 2) in all normal vessels examined ($n=18$). The sarcoplasmic reticulum (appearing blackened by

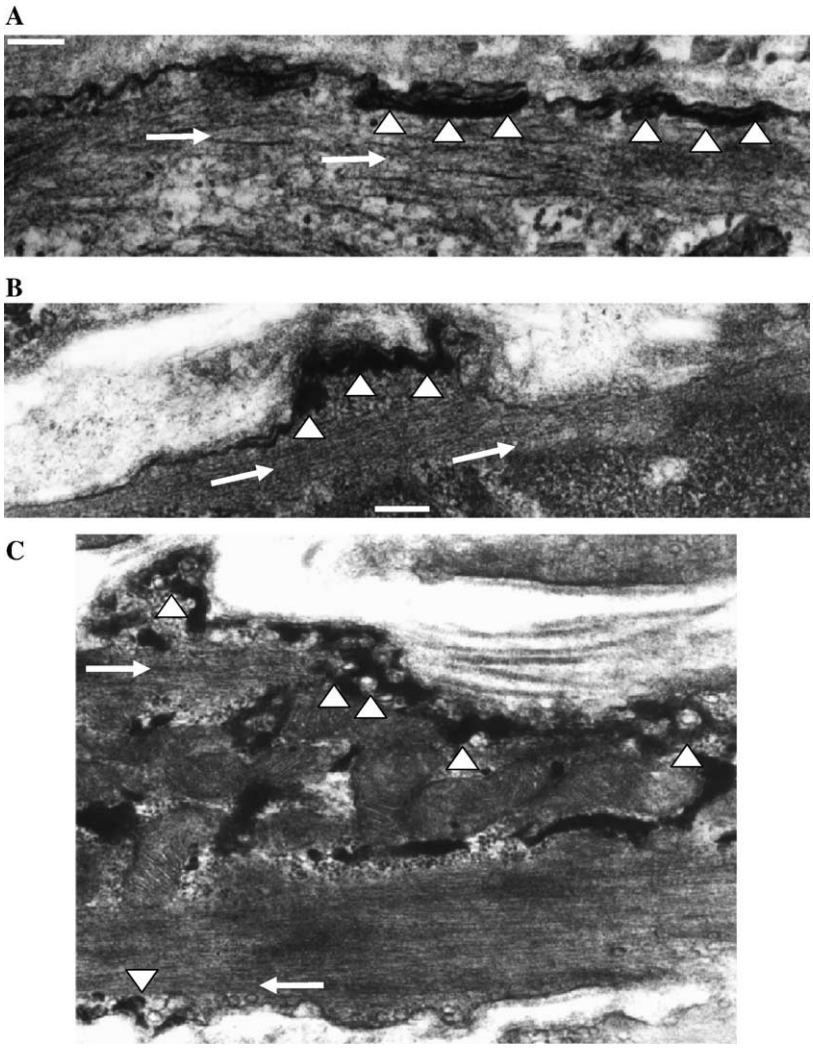

Fig. 6. Effects of mβcd treatment and cholesterol replenishment on smooth muscle plasma membrane structure. (A, B) Following mβcd treatment caveolae are absent even though peripheral SR localisation close to the plasmalemma remains visible. (C) Shows smooth muscle ultrastructure of an artery which received cholesterol supplementation following mβcd treatment. Here the peripheral SR is in close association with caveolae. Scale bars=200 nm.

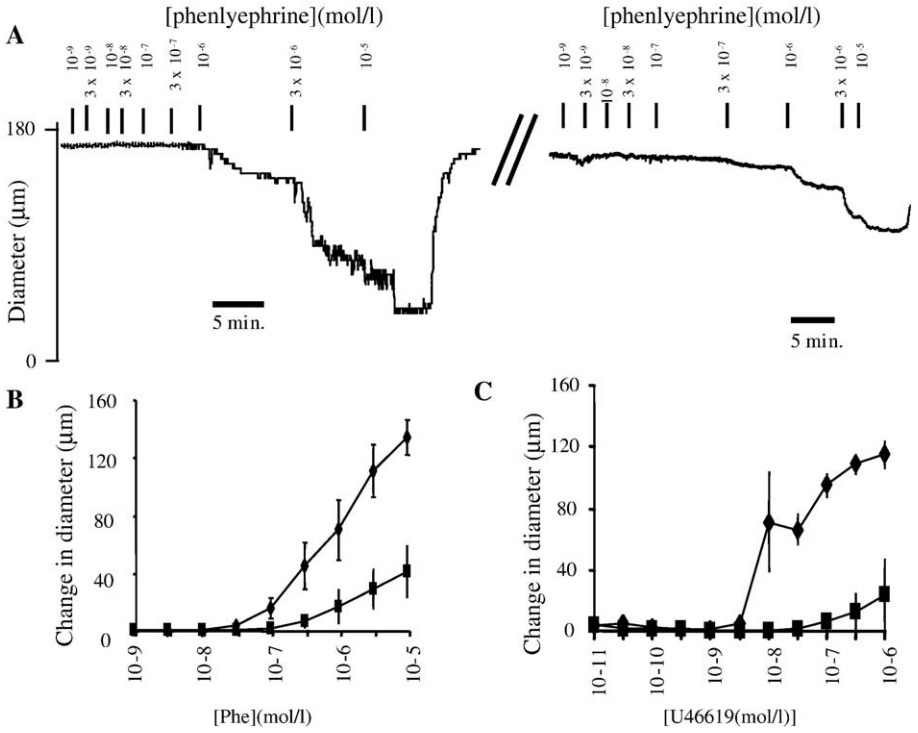

Fig. 7. The influence of mβcd treatment on agonist-sensitivity. (A) Representative tracing of phenylephrine concentration–diameter responses before and after mβcd treatment. B and C show that dose-responsiveness to phenylephrine or U44619 is blunted in pressurised arteries after mβcd treatment.

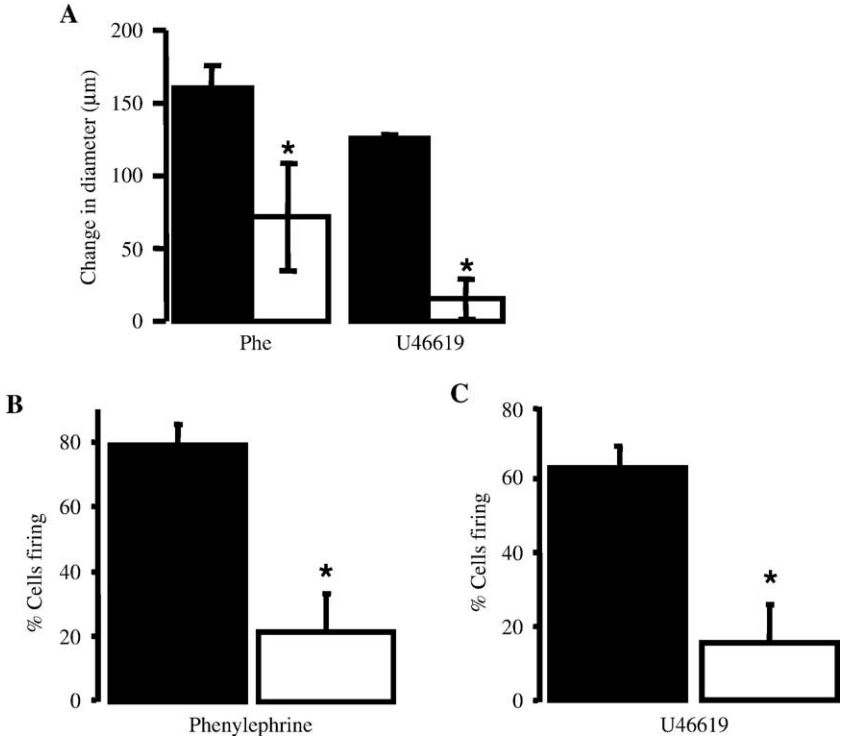

Fig. 8. Mβcd effects on pressurised artery diameter and on smooth muscle $[Ca^{2+}]_i$ oscillations. (A) Diameter reductions to maximal doses of phenylephrine and U44619 were less after mβcd treatment (160±14 μm before and 72±37 μm after for phenylephrine; 126±2.4 μm before and 15±13 μm after for U46619). (B) The blunted responsiveness following mβcd treatment is accompanied by a reduction in the percentage of cells exhibiting Ca^{2+} oscillations in response to 3×10^{-7} mol/l phenylephrine (79±6.2%, $n=3$ cells from 6 vessels before (black box) and 22±12%, $n=88$ cells from 6 vessels after) or U46619 (63±5.8%, $n=172$ cells from 11 vessels before (black box) and 16±10%, $n=45$ cells from 5 vessels after).

OsFeCN staining) when evident at the cell periphery was observed in close proximity to caveolar domains in 13 of 18 vessels. However, not all caveolar regions were associated with peripheral SR. Abundant SR staining was also noted in the centre of cells near to mitochondria and the nucleus. The location of the nucleus, central SR and mitochondria in the middle of the cell could be explained by the enveloping of these organelles by the tightly packed myofilaments running parallel to the longitudinal axis of the cell (Fig. 1). These arrangements occurred in both vessels fixed whilst relaxed ($n=5$, Fig. 2) and in vessels constricted with maximal doses of U46619 ($n=7$, Fig. 1), phenylephrine ($n=3$) or high K^+ ($n=3$). Interestingly, even though the central SR was generally enveloped by the myofilament lattice, occasional strands of peripheral SR are seen to course from caveolar regions deeper through the cell forming a direct link to the central SR (indicated by asterisks in Fig. 1).

In magnified sections the peripheral SR could be seen to approach to within 10–20 nm of the plasma membrane; this positioning could be observed in a continuum along lengths of membrane up to 1.5 μm in the same plane of section (Fig. 2). Also, in regions of the plasma membrane enriched in caveolae, the periperal SR was found to encircle these invaginations (Fig. 2). This caveolae–peripheral SR region was also closely arranged next to the myofilament lattice running parallel to the axis of the plasma membrane.

3.2. Bi-directional Ca^{2+} oscillations in smooth muscle cells of pressurised arteries

Stimulation with the G-protein-coupled receptor agonists (phenylephrine or U46619) resulted in vessel diameter reductions that were accompanied by smooth muscle Ca^{2+} oscillations that were asynchronous between neighbouring cells. Typically, these oscillations took the form of a Ca^{2+} wave originating in one region of the cell and propagating along the length of the rest of the cell (up to 70 μm length visualised) (Fig. 3). However, this did not indicate a unique directionality to the Ca^{2+} wavefront. In 11 vessels, a Ca^{2+} wave could be seen to proceed in one direction along the length of a cell and, in later acquisitions of the same cell, another Ca^{2+} wave originated in a different region and propagated in the opposite direction along the longitudinal axis of the cell (Fig. 3B–D). In 4 vessels, there was also evidence of elevations in Ca^{2+} in two distinct parts of the cell that propagated towards each other and 'collided' (Fig. 3E). Only in one vessel was a Ca^{2+} wave observed to originate near the middle of the cell and progress away from the point of origin in both directions along the cell. These findings suggest that the origins of a Ca^{2+} wave are usually towards the ends of the cell distant from the middle portion. This is further supported by circumstances (5 vessels) where the propagated Ca^{2+} wave clearly avoided the nucleoplasm (not shown).

3.3. Functional and ultrastructural effects of calyculin-A or mβcd on pressurised resistance arteries

Calyculin-A treatment of isobaric rat mesenteric small arteries (Fig. 4A) resulted in the development of maximal tonic constrictions that were of even greater magnitude (change in diameter 178.0±8.3 μm) than those to maximal phenylephrine in the same vessels (107.3±25.3 μm; $p<0.05$). The calyculin-A constrictions were irreversible in the subsequent 15 min washout period. These maximum maintained contractions to calyculin-A occurred even in the absence of extracellular Ca^{2+} in two experiments (Fig. 4A). Furthermore, when compared to the magnitude of global Ca^{2+} changes induced by high K^+ stimulation, calyculin-A treatment did not significantly (0.15±0.10-fold of high K^+) alter basal Ca^{2+} (Fig. 4B). However, calyculin-A treatment resulted in significantly fewer cells undergoing oscillations in Ca^{2+} at rest or following stimulation with one of two G-protein-coupled receptor agonists (phenylephrine or U46619) compared to before treatment (Fig. 4C). Consistent with this, the elevation in global Ca^{2+} in response to maximal dose of phenylephrine following calyculin-A treatment was 47+26% ($n=3$) of that to phenylephrine before calyculin-A.

All the fixed calyculin-A-treated arteries examined electron microscopically ($n=7$) exhibited different features from untreated arteries (Fig. 5). Regions of the hyperconstricted arteries had the appearance of prominent notches. These were enriched in caveolae but the SR was no longer in such close juxtaposition with the invaginations. Rather, the peripheral SR was arranged in concentric swirls that were not apparent in untreated tissues. On some occasions the caveolae appeared to have become invaginated/fused with these altered SR structures (e.g. Fig. 5). Such gross rearrangements were not observed in any of the calyculin-A untreated vessels that had been fixed whilst constricted with physiological stimuli.

Electron microscopic examination of the smooth muscle cells following treatment with the cholesterol binding drug mβcd ($n=10$) indicated flattened plasma membranes with few caveolae even though, in many cases, peripheral SR coupling close to the plasmalemma could still be observed in the absence of caveolae (Fig. 6A–B, $n=6$). In mβcd-treated arteries supplemented with water soluble cholesterol this was not the case—here, caveolae and peripheral SR close associations could still be observed (Fig. 6C). Mβcd treatment also resulted in a blunting of the arterial responses to agonist stimulation (Figs. 7 and 8). This was partly reversed by supplementation with water soluble cholesterol (mean diameter changes to phenylephrine were 158±16 μm control, 50±19 μm after mβcd and 86±18 μm following cholesterol supplementation ($p<0.05$)). As in calyculin-A-treated arteries, mβcd treatment also resulted in a reduction of the number of cells exhibiting Ca^{2+} oscillations to stimulation with either phenylephrine or U46619 (Fig. 6D–E).

4. Discussion

In this study, we have performed a structural and functional analysis of the relationship between caveolae and the peripheral SR in smooth muscles of resistance arteries. Electron microscopy revealed that the peripheral SR often enshrouds individual caveolae resulting in a close association of the two membrane structures. The possible implications of this arrangement for the regulation of vessel tone were evidenced by the actions of calyculin-A and mβcd.

Calyculin-A, an inhibitor of serine/threonine phosphatases, maximally constricted vessels both in the presence and absence of extracellular Ca^{2+} consistent with a mechanism of action attributable to inhibition of myosin phosphatase activity. This produced a rearrangement of the peripheral SR–caveolae distribution with prominent notches of membrane containing condensed caveolae and peripheral SR. The SR now appeared as tight swirls and no longer as intimately associated with rows of caveolae. These notched regions of the cell were not immediately overlying the myofilament lattice as in untreated cells. Caveolae in a number of cell types have been reported to be internalised by phosphatase inhibition [28–30]. The fact that agonist-mediated Ca^{2+} oscillations were reduced in treated arteries is in agreement with the suggestion of Lee et al., in venous smooth muscle [27], that the caveolae–peripheral SR arrangements disrupted by calyculin-A are normally important for the generation of Ca^{2+} oscillations.

Mβcd treatment resulted in a disruption of caveolae and a reduction in agonist-mediated constrictions. Thus, in common with calyculin-A-treated tissues, the caveolar–peripheral SR close association was disrupted although the SR remained in close apposition to flattened areas of the plasmalemma. Nonetheless, agonist-mediated Ca^{2+} oscillations were again reduced providing further indirect evidence supporting an important role for caveolae–SR couplings in the origin of Ca^{2+} oscillations. However, one must be cautious in the interpretation as changes in receptor distribution or Ca^{2+} entry may occur with mβcd treatment [8,9]. Nonetheless, in addition to pressurised vessels reported here, calyculin-A or mβcd treatment has resulted in alteration of smooth muscle Ca^{2+} oscillations [8,12,27].

A burgeoning body of evidence suggests that resistance arteries responded to G-protein-coupled contractile stimuli with waves of Ca^{2+} propagating along the length of individual smooth muscle cells [14,18,26,33]. As indicated in the data presented here, the Ca^{2+} oscillations are not unidirectional; on occasions when there was more than one discreet point of origin of Ca^{2+} waves in the same cell, the waves were observed to progress in opposite directions. In isolated smooth muscle cells, and intact smooth muscle tissues, such Ca^{2+} oscillations are disrupted by modulators of SR Ca^{2+} homeostasis, including inhibitors of calcium-induced Ca^{2+} release or IP_3-sensitive Ca^{2+} release [[21–23,26] suggesting a dependence on regenerative SR Ca^{2+} release [19,34]. This suggests that the progression of a Ca^{2+} wave will be dependent upon the intracellular arrangement of the SR.

The separation of the peripheral SR and the caveolar plasma membrane of only ~10–20 nm may give rise to so-called focal discharge sites underlying Ca^{2+} spark activity in mesenteric and other smooth muscles [20,35–37]. Agonist-mediated Ca^{2+} waves appear to originate at focal discharge/Ca^{2+} spark sites, although controversy exists as to whether summation or inhibition of sparks contributes to cellular Ca^{2+} waves [20,26]. In several regions of a cell, peripheral SR strands were found to connect with more centrally located SR that, in turn, followed a course along the longitudinal axis of the cell in proximity to the nuclear membrane and mitochondria. The appearance of several focal discharge sites per cell [37] could arise from multiple caveolae–peripheral SR couplings, and together with a peripheral–central SR continuum, may explain the observations of Ca^{2+} waves (i) propagating away from that site along the longitudinal axis of the cell and (ii) not necessarily being unidirectional. The latter would offer the advantage of Ca^{2+} wave generation occurring in response to extraneous excitatory stimuli that might originate at quite distant (feasibly > 100 μm) plasmalemmal sites. Future experiments with better spatial and temporal resolution will be required to directly confirm this possibility.

Caveolae–peripheral SR couplings, and portions of central SR along the longitudinal axis of the cell, are closely positioned adjacent to the tightly packed myofilaments. A major implication of these arrangements is that any elevations in Ca^{2+} as a result of propagated waves from the SR will likely activate the myofilaments that are in close proximity. Notably, myosin light chain kinase and a proportion of calmodulin—proteins essential for Ca^{2+}-dependent contractile activation—are tightly bound to the myofilaments [38,39].

In summary, a close structural link between caveolae and peripheral SR exists in pressurised rat mesenteric arteries similar to that reported for guinea pig aorta, vas deferens [32,39,40], bladder [27] and human arteries [41]. Disruption of the caveolae–SR associations with the underlying myofilament lattice can be invoked by calyculin-A or mβcd treatment with a consequent impairment of Ca^{2+} oscillations and function. These data, together with an increasing body of evidence suggesting localisation of proteins involved in Ca^{2+} homeostasis to caveolar–SR domains [3,5–11], support a role for caveolae in the generation of Ca^{2+} oscillations and development of vascular tone. Future studies investigating (i) the immunogold localisation for IP3 and/or ryanodine receptor [5,29,37] close to caveolae and (ii) Ca^{2+} and tone changes in vessels of caveolin knockout mice will be instructive in this matter.

Acknowledgements

Supported by the British Heart Foundation and Tommy's, the Baby Charity.

References

[1] Taggart M. Smooth muscle excitation–contraction coupling: a role for caveolae and caveolins? NIPS 2001;16:61–5.

[2] Bergdahl A, Sward K. Caveolae-associated signalling in smooth muscle. Can J Physiol Pharmacol 2004;82:289–99 [& Sward].

[3] Moore ED, Voigt T, Kobayashi YM, Isenberg G, Fay FS, Gallitelli MF, et al. Organization of Ca^{2+} release units in excitable smooth muscle of guinea-pig urinary bladder. Biophys J 2004;87:1836–47.

[4] Je HD, Gallant C, Leavis PC, Morgan KG. Caveolin-1 regulates contractility in differentiated vascular smooth muscle. Am J Physiol 2003;286:H91–8.

[5] Fujimoto T, Nakade S, Miyawaki A, Mikoshiba K, Ogawa K. Localisation of inositol 1,4,5-triphosphate receptor-like protein in plasmalemmal caveolae. J Cell Biol 1992;119:1507–13.

[6] Fujimoto T. Calcium pump of the plasma membrane is localized in caveolae. J Cell Biol 1993;120:1147–57.

[7] Brainard AM, Miller AJ, Martens JR, England SK. Maxi-K channels localize to caveolae in human myometrium: a role for an actin–channel–caveolin complex in the regulation of myometrial smooth muscle K^+ current. Am J Physiol 2005;289:C49–57.

[8] Dreja K, Voldstedlund M, Vinten J, Tranum-Jensen J, Hellstrand P, Sward K. Cholesterol depletion disrupts caveolae and differentially impairs agonist-induced arterial contraction. Arterioscler Thromb Vasc Biol 2002;22:1267–72.

[9] Berghal A, Gomez MF, Dreja K, Xu S, Adner M, Beech DJ, et al. Cholesterol depletion impairs vascular reactivity to endothelin-1 by reducing store-operated Ca^{2+} entry dependent on TrpC1. Circ Res 2003;93:839–47.

[10] Cho WJ, Daniel EE. Proteins of interstitial cells of Cajal and intestinal smooth muscle, colocalized with caveolin-1. Am J Physiol 2005;288: 571–85.

[11] Darby PJ, Daniel EE. Caveolae from canine airway smooth muscle contain the necessary components for a role in Ca^{2+} handling. Am J Physiol 2000;279:L1226.

[12] Lohn M, Furstenau M, Sagach V, Elger M, Schulze W, Luft FC, et al. Ignition of Ca sparks in arterial and cardiac muscle through caveolae. Circ Res 2000;87:1034–9.

[13] Iino M, Kasai H, Yamazawa T. Visualisation of neural control of intracellular Ca^{2+} concentration in single vascular smooth muscle cells in situ. EMBO J 1994;13:5026–31.

[14] Miriel VA, Mauban JRH, Blaustein MP, Wier GW. Local and cellular Ca^{2+} transients in smooth muscle of pressurized rat resistance arteries during myogenic and agonist stimulation. J Physiol 1999;518:815–24.

[15] Jaggar JH, Nelson MT. Differential regulation of Ca^{2+} sparks and Ca^{2+} waves by UTP in rat cerebral artery smooth muscle cells. Am J Physiol 2000:C1528–39.

[16] Lee CH, Poburko D, Sahota P, Sandhu J, Ruehlmann DO, Van Breeman C. The mechanism of phenylephrine-mediated $[Ca^{2+}]_i$ oscillations underlying tonic contraction in the rabbit inferior vena cava. J Physiol 2001;534:641–50

[17] Peng H, Matchkov V, Ivarsen A, Aalkjaer C, Nilsson H. Hypothesis for the initiation of vasomotion. Circ Res 2001;88:810–5.

[18] Shaw L, O'Neill SC, Jones CJP, Austin C, Taggart MJ. Comparison of U46619-, endothelin-1- or phenylephrine-induced changes in cellular Ca^{2+} profiles and Ca^{2+}-sensitisation of constriction of pressurised rat resistance arteries. Br J Pharmacol 2004;141:678–88.

[19] Lee CH, Poburko D, Kuo K, Seow Y, Van Breeman C. Ca^{2+} oscilations, gradients, and homeostasis in vascular smooth muscle. Am J Physiol 2002:H1571–83.

[20] Bolton TB, rdienko V, Povstyan VO, Harhun MI, Pucovsky V. Smooth muscle cells and interstitial cells of blood vessels. Cell Calcium 2004;35:643–57.

[21] White C, McGeown JG. Carbachol triggers RyR-dependent Ca^{2+} release via activation of IP_3 receptors in isolated rat gastric myocytes. J Physiol 2002;542:725–33.

[22] Gordienko DV, Bolton TB. Crosstalk between ryanodine receptors and IP_3 receptors as a factor shaping spontaneous Ca^{2+} release events in rabbit portal vein myocytes. J Physiol 2002;542:743–62.

[23] McCarron JG, MacMillan D, Bradley KN, Chalmers S, Muir TC. Origin and mechanisms of Ca^{2+} waves in smooth muscle as revealed by localised photolysis of caged inositol 1,4,5-triphosphate. J Biol Chem 2004;279:8417–27.

[24] Zhang WJ, Balke CW, Wier WG. Graded α_1-adrenoceptor activation of arteries involves recruitment of smooth muscle cells to produce 'all or none' Ca^{2+} signals. Cell Calcium 2001;29:327–34.

[25] Jaggar H. Intravascular pressure regulates local and global Ca^{2+} signalling in cerebral artery smooth muscle cells. Am J Physiol 2001;281:C439–48.

[26] Lamont C, Weir G. Different roles of ryanodine receptors and inositol (1,4,5)-triphosphate receptors in adrenergically stimulated contractions of small arteries. Am J Physiol 2004;287:H617–25.

[27] Lee C, Kuo K, Dai J, Leo JM, Seow CY, Van Breeman C. Calyculin-A disrupts subplasmalemmal junction and recurring Ca^{2+} waves in vascular smooth muscle. Cell Calcium 2005;37:9–16.

[28] Parton RG, Joggesrt B, Simons K. Regulated internalization of caveolae. J Cell Biol 1994;127:1199–215.

[29] Thomsen P, Roepstorff K, Satlhult M, van Deurs B. Caveolae are highly immobile plasma membrane microdomains, which are not involved in constitutive endocytotic trafficking. Mol Cell Biol 2002; 13:238–50.

[30] Kiss, AL, Botos, E, Turi, A, Mullner, N. Okadaic acid treatment causes tyrosine phosphorylation of caveolin-2 and induces internalisation of caveolae in rat peritoneal macrophages.

[31] Forbes MS, Plantholt BA, Sperelakis N. Cytochemical staining procedures selective for sarcotubular systems of muscle: modifications and applications. J Ultrastruct Res 1977;60:306–27.

[32] Nixon GF, Mignery GA, Somlyo AV. Immunogold localization of inositol 1,4,5-trisphosphate receptors and characterization of ultra-structural features of the sarcoplasmic reticulum in phasic and tonic smooth muscle. J Muscle Res Cell Motil 1994;15:682–700.

[33] Mauban JRH, Lamont C, Balke W, Wier GW. Adrenergic stimulation of rat resistance arteries affects Ca^{2+} sparks, Ca^{2+} waves, and Ca^{2+} oscillations. Am J Physiol 2001;280:H2399–405.

[34] Berridge M. The endoplasmic reticulum: a multifunctional signalling organelle. Cell Calcium 2002;32:235–49.

[35] Pucovsky V, Gordienko DV, Bolton TB. Effect of nitric oxide donors and noradrenaline on Ca^{2+} release sites and global intracellular Ca^{2+} in myocytes from guinea-pig small mesenteric arteries. J Physiol 2002;539:25–39.

[36] Cheranov SY, Jagger JH. Mitochondrial modulation of Ca^{2+} sparks and transient Kca currents in smooth muscle cells of rat cerebral arteries. J Physiol 2004;556:755–71.

[37] Zhuge, R, Fogarty, KE, Baker, SP, McCarron, JG, Tuft, RA, Lifshitz, LM, Walsh, JV. Ca^{2+} spark sites in smooth muscle cells are numerous and differ in number of ryanodine receptors, large conductance K^+ channels, and coupling ratio between them. Am J Physiol 287: C1577–88.

[38] Lin P, Luby-Phelps K, Stull JT. Binding of myosin light chain kinase to actin myosin filaments. J Biol Chem 1997;272:7412–20.

[39] Wilson DP, Sutherland C, Walsh MP. Ca^{2+} activation of smooth muscle contraction: evidence for the involvement of calmodulin that is bound to the triton insoluble fraction even in the absence of Ca^{2+}. J Biol Chem 2002;277:2186–92.

[40] Lesh RE, Nixon GF, Flesicher S, Airey JA, Somlyo AP, Somlyo AV. Localisation of ryanodine receptors in smooth muscle. Circ Res 1998;82:175–85.

[41] Sweeney, M, Jones, CJ, Greenwood, SL, Baker, PN, Taggart, MJ. Ultrastructural features of smooth muscle and endothelial cells of isolated isobaric human placental and maternal arteries. Placenta Epub ahead of print. doi:10.1016/j.placenta.2005.05.010.